12th Int. Particle Acc. Conf. IPAC2021, Campinas, SP, Brazil JACoW Publishing
ISBN: 978-3-95450-214-1 ISSN: 2673-5490 doi:10.18429/JACoW-IPAC2021-MOPAB087

DESIGN OF A MULTI-BUNCH FEEDBACK KICKER IN SPEAR3*

K. Tian†, J. Langton, N. Parry, J. Safranek, J. J. Sebek
SLAC National Accelerator Laboratory, Menlo Park, California, USA

Abstract

The new multi-bunch feedback kickers have been designed for SPEAR3 to replace the current device loaned from ALS. In this paper, we first present the specification of the kickers based on the beam physics requirements. Then the mechanical design of the kicker is elaborated. Next we present numerical simulations, both in the time and frequency domains, that we conducted to evaluate the shunt impedance and beam coupling impedance of the kicker. We also used the simulation results to estimate the surface heating induced from the beam and the external source.

INTRODUCTION

A multi-electrode stripline is a useful beam instrumentation and control device and has been installed in nearly every modern synchrotron radiation storage ring for various applications. Acting as a pickup device or a kicker, the beam dynamics due to the interaction between the beam and such a device has been well studied and understood [1]. This has been particularly beneficial to the design of stripline kickers for a transverse multi-bunch feedback (TMBF) system, where they often serve as the actuators. The SPEAR3 TMBF system [2] is equipped with digital processing units from Dimtel [3], two 500 W broadband RF amplifiers, and a stripline kicker. The system is a crucial part of the machine protection system and has been proved to be sufficient to control beam instabilities. However, stronger kickers are desirable for new capabilities such as bunch cleaning and demanding accelerator physics projects such as resonant crabbing. The design process of a kicker is normally an optimization process for multiple objectives, such as shunt impedance, beam coupling impedance, and manufacturability for building and maintaining the device. Based on the individual requirements of different facilities, distinct priorities and trade-offs have been chosen when kickers for various machines were designed. We have carefully reviewed the design of kickers from different facilities [4–10] and compared some of them in numerical simulations. In the end, we adopted most of the features in the MAX IV design but developed different approaches in manufacturing the actual device.

PHYSICS SPECIFICATIONS

With the new TMBF kicker, we want to meet the requirements for potential future needs, such as bunch cleaning and resonant crabbing, an R&D project that requires the ability to drive a single bunch with a strong kick.The main requirements for the kickers are listed as the following:

Shunt Impedance R_{sh}: We require the kicker shunt impedance to be larger than 10 kΩ at 238.155 MHz.

Loss Factor k_l: We would like to keep the contribution from the kicker below 1% of the total loss factor of the ring, i.e. 0.06 V/pC.

Transverse Impedance: The horizontal and vertical coupled bunch instability (CBI) thresholds, when only considering radiation damping, for SPEAR3 are: $Z_x = 0.3\ \mathrm{M}\Omega/\mathrm{m}$ and $Z_y = 0.5\ \mathrm{M}\Omega/\mathrm{m}$.

Electrode Length: The length of the electrode (distance between the upstream beam feedthrough and downstream beam feedthrough) is determined by the SPEAR3 RF frequency and should be 314.9 mm.

MECHANICAL DESIGN

SPEAR3 will install two identical TMBF kickers, one for each plane. They will conform to the physics specifications while meeting several mechanical goals. These goals include, but are not limited to, robust structures and elements specifically with regard to feedthroughs, serviceable assembly methodology to accommodate repairs or upgrades, and a conservative approach to cooling of the electrodes. After multiple iterations of the design, we have converged to a kick design resembling many geometric features of the MAX IV TMBF kickers, but with different approaches to assembling and machining the actual structure.

As shown in Fig. 1 , the electrodes are concentric with the chamber. Two ribs are mounted to better match the characteristic impedance for both the even and odd operating modes. The end design is more complex due to the importance in minimizing the beam coupling impedance. The final design for the kicker ends includes end caps (blue), back tapers (purple), and electrode tapers (red). The dimensions of these parts were carefully picked from numerical electromagnetic simulations to optimize the kicker performance. The tapered electrodes are designed to reduce the beam coupling impedance at high frequency. To maintain smooth and reasonably constant gaps between the electrode and the rest of the structure, the taper here is more complex than a simple linear curve. The assembly of end caps, back tapers, and electrodes in the chamber is illustrated in Fig. 2. The end cap meets the chamber ribs to maintain the nearly constant gap to the electrodes. The back taper has a conical slope blending into the chamber inner wall and is fit into the end cap. The electrodes are made of aluminum and other parts are made of stainless steel. However, all surfaces seen by the beam will be copper plated to reduce the resistive wall heating.

---

* Work supported by U.S. Department of Energy under Contract No. DE-AC02-76SF00515. This research used resources of the National Energy Research Scientific Computing Center (NERSC), a U.S. Department of Energy Office of Science User Facility operated under Contract No. DE-AC02-05CH11231.

† ktian@slac.stanford.edu

ISBN: 978-3-95450-214-1 ISSN: 2673-5490 doi:10.18429/JACoW-IPAC2021-MOPAB087

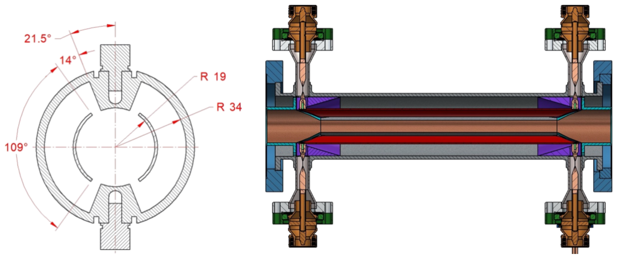

Figure 1: Overview of the TMBF kicker design: the cross section of the nominal section (left) and the cut away view of the whole structure (right).

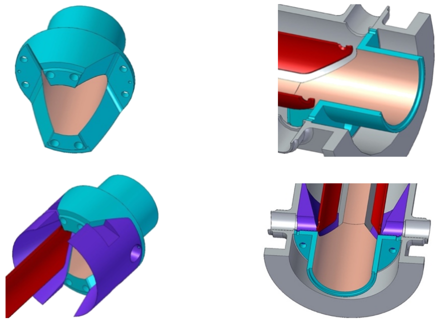

Figure 2: Detailed view of the end design: the end cap (top left); placement of the end cap and the electrodes with the chamber rib (top right); adding back tapers (bottom left); complete end design (bottom right).

NUMERICAL SIMULATIONS

The physics design of the TMBF kicker involves multiple step simulations with both 2D and 3D software. Poisson [11], a well-known 2D electrostatic solver, was used to calculate the characteristic impedance for both even and odd modes, as well as the geometric factor for different transverse geometries. We set up routines to scan the geometric parameters using Poisson simulations. Based on the scanning results, we chose from multiple sets of designs with good balance between high geometric factors for a strong kick and good matching for characteristic impedance. Then, in order to characterize the beam coupling impedance as well as the shunt impedance with kicker transitions, 3D simulations using several codes in ACE3P code suites [12] were carried out at NERSC [13]. T3P, a time domain finite element code, was used for calculations of short/long range wake fields as well as for RF heating. Omega3P is an eigenmode solver for calculating the beam coupling impedance of the trapped higher order modes (HOMs). S3P provides s-parameter simulations, which determine the matching condition and kicker shunt impedance.

Simulation Model

We depict both the 2D and 3D simulation models in Fig. 3. In the Poisson model, b and t represent the chamber radius and the thickness of the electrodes, respectively. φ_s, φ_g, and φ_r represent the covering angle of one electrode, the angle of the gap between the electrode and the rib, and the half coverage angle of a chamber rib, respectively. There are many numerical choices of transverse geometry that can satisfy the specifications. After comparing many of them with 2D and 3D simulations, three designs, our 11i, 11j, and 11f designs, were chosen as candidates to be built. All three designs share the same dimension for the electrode radius a, chamber radius b, and electrode thickness t. However, slightly different covering angle for the rib and electrode lead to slightly different characteristic impedances for the even and odd modes and geometry factors, which are compared in Table 1, where Z_{odd}/Z_{even} is the odd/even mode characteristic impedance and g is the geometry factor. As will be discussed later, design 11j was chosen for production due to its slightly larger shunt impedance.

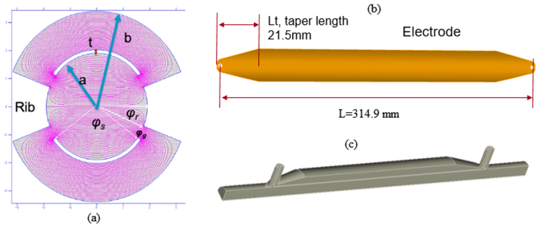

Figure 3: Numerical models for 2D and 3D simulations: (a), Poisson model; (b), the electrode in the 3D model; (c), the 3D model.

Table 1: Design Comparison for SPEAR3 MBF Kickers

	$\varphi_s/\varphi_g/\varphi_r$	$Z_{odd}(\Omega)$	$Z_{even}(\Omega)$	g
11j	109° /14° /21.5°	47.0	53.2	1.11
11i	106° /12° /25°	46.6	51.9	1.084
11f	106° /10°/27°	45.0	49.8	1.075

Shunt Impedance

The kicker shunt impedance can be estimated using Lambertson's formula [1] using a 2-D approximation. With transitions at both ends, the actual results will be different and require 3D simulations. The definition of the shunt impedance from a circuit model is $R_{sh} = V_\perp^2/2P$, where $V_\perp$ is the vertical deflecting voltage, and P is the input driving power. The deflecting voltage can be calculated from electromagnetic fields determined by S3P. In Fig. 4, the shunt impedances are compared for all three designs. As indicated in Table 1, the design with the larger odd mode characteristic impedance and geometric factor has higher shunt impedance throughout the spectrum, although the difference decreases for higher frequency. The dashed line in the figure is calculated using Lambertson's formula assuming $Z_{odd} = 50\ \Omega$, $g = 1.1$, and $a = 19$ mm. The estimated shunt impedance for the ALS kicker currently installed in SPEAR3 is also plotted. Although all three designs meet the specification of 10 kΩ at 238.155 MHz, design 11j is preferable in terms of shunt impedance.

ISBN: 978-3-95450-214-1 ISSN: 2673-5490 doi:10.18429/JACoW-IPAC2021-MOPAB087

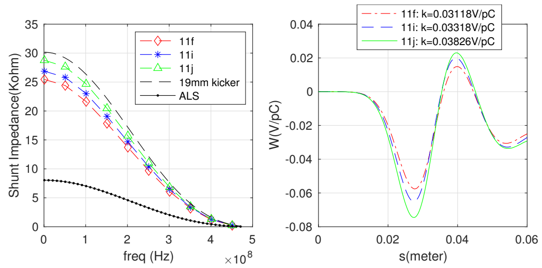

Figure 4: Shunt impedance (left) and loss factor (right).

Loss Factor

The main beam effects from the short range wakefields is in the longitudinal loss factor, which can be directly calculated using T3P in the time domain. We compare these results for the three design in Fig. 4. The wake potentials along the bunch and the loss factors are slightly different for each design: 0.0312 V/pC for 11f, 0.0332 V/pC for 11i, and 0.0383 V/pC for 11j. Comparing the shunt impedance for each design, the trade-off between higher shunt impedance and lower loss factor is clearly shown for this type of kicker design.

Trapped Modes

We calculated the beam impedance using frequency domain simulations to solve all supporting HOMs. As expected, for a vertical kicker, the vertical modes are mostly damped due to the coupling from the feedthrough, but there are several horizontal modes which cannot be coupled out. However, as shown in Fig. 5, for all three designs, the impedances of all modes are below the threshold of 0.3 MΩ/m. Since the beampipe cut off frequency is below 5 GHz, no modes above that frequency can be trapped in the kicker structure. Again, the results show the small trade-off between shunt impedance and beam impedance. Simulation results from T3P for the impedance spectrum up to 10 GHz for the horizontal and transverse modes was also checked. The resonant peaks agree with the mode calculations from Omega3P.

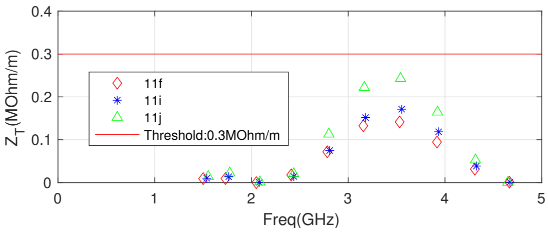

Figure 5: Trapped horizontal modes in the vertical kicker.

RF Heating

We conducted time domain simulations in T3P and evaluated the time-resolved surface power loss using the magnetic field on the surface grids and the surface resistance of the boundary materials. Figure 6 shows the time-resolved power dissipation on the stainless steel chamber wall and the copper plated surfaces within the first 8 ns after the beam enters the structure. By integrating the surface power over time, one can then estimate the surface power loss for a particular bunch fill pattern. However, one constraint for this calculation is that we can only specify a fixed frequency when calculating the surface resistance. We pick 1 GHz for ease of scaling. Neglecting the coupling effects from bunch to bunch, we can estimate the heating power from all bunches by summing up the contribution from each individual bunch. The calculation results show that, out of the total beam power loss of about 27 W, only about 0.72 W will dissipate on the surfaces of the kicker.

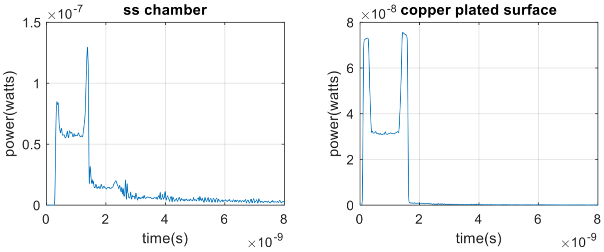

Figure 6: Surface power dissipation for kicker design 11j.

Other Simulations

We have carried out S-parameter simulations using S3P and the results confirmed good matching of the kicker design. To study the impact of mechanical tolerance for assembling the electrodes, we simulated the kicker model with 0.5 degree rotation error on the electrodes and the model with 1 mm error in the longitudinal position of the electrodes. We also conducted simulations with mismatched feedthrough. All results confirmed that the beam coupling impedance would still stay below the threshold even with these errors.

CONCLUSION

The new SPEAR3 multi-bunch feedback kicker design is driven by the physics specifications of having a high shunt impedance and low loss factors. To achieve these goals, we adopt many features of the MAX IV kicker and develop an innovative mechanical design for a device to manufacture and service. Extensive simulation studies have been conducted to characterize the performance of the kicker and investigate any possible beam impedance problems. The studies indicate the design meets all of our requirements.

ACKNOWLEDGEMENTS

We would like to thank C. Ng and L. Xiao for supporting the ACE3P codes. We also want to acknowledge W. Cheng, H.O.C. Duarte, S. Santis, G. Rehm, and D. Olsson for providing their kicker design and providing constructive advice. Finally, we thank J. Sarayi and J. Dickey for their efforts in building the kicker.

REFERENCES

[1] D. A. Goldberg and G. R. Lambertson, "Dynamic devices a primer on pickups and kickers", in *AIP Conference Proceedings*, vol. 249, p. 537 Jul. 2018. `doi.org/10.1063/1.41979`

[2] K. Tian *et al.*, "Commission of the Transverse Bunch-by-Bunch Feedback at SPEAR3", in *Proc. 10th Int. Particle Accelerator Conf. (IPAC'19)*, Melbourne, Australia, May 2019, pp. 4081–4084. `doi:10.18429/JACoW-IPAC2019-THPRB112`

[3] Dimtel, http://www.dimtel.com

[4] W. X. Cheng, A. Blednykh, S. Krinsky, and O. Singh, "Stripline Kicker Design for NSLS2 Storage Ring", in *Proc. 24th Particle Accelerator Conf. (PAC'11)*, New York, NY, USA, Mar.-Apr. 2011, paper MOP266, pp. 603–605.

[5] H. O. C. Duarte and S. R. Marques, "Impedance Optimization of Sirius Stripline Kicker", in *Proc. 4th Int. Beam Instrumentation Conf. (IBIC'15)*, Melbourne, Australia, Sep. 2015, pp. 302–306. `doi:10.18429/JACoW-IBIC2015-TUPB006`

[6] H. O. C. Duarte, L. Liu, and S. R. Marques, "Evaluation and Attenuation of Sirius Components Impedance", in *Proc. 8th Int. Particle Accelerator Conf. (IPAC'17)*, Copenhagen, Denmark, May 2017, pp. 3048–3051. `doi:10.18429/JACoW-IPAC2017-WEPIK054`

[7] J. N. Corlett, J. Johnson, G. Lambertson, and F. Voelker, "Longitudinal and Transverse Feedback Kickers for the ALS", in *Proc. 4th European Particle Accelerator Conf. (EPAC'94)*, London, UK, Jun.-Jul. 1994, pp. 1625–1628.

[8] C. Mariette, J.-C. Denard, and R. Nagaoka, "Excitation Striplines for SOLEIL Fast Transverse Feedback", in *Proc. 8th European Workshop on Beam Diagnostics and Instrumentation for Particle Accelerators (DIPAC'07)*, Venice, Italy, May 2007, paper WEPC16, pp. 343–345.

[9] D. Olsson, L. Malmgren, and K. Ahnberg, "Design and Implementation of Stripline Feedback Kickers in the MAX IV 3 GeV Ring", in *Proc. 8th Int. Particle Accelerator Conf. (IPAC'17)*, Copenhagen, Denmark, May 2017, pp. 4285–4288. `doi:10.18429/JACoW-IPAC2017-THPIK086`

[10] C. Belver-Aguilar, A. Faus-Golfe, F. Toral, and M. J. Barnes, "Stripline design for the extraction kicker of Compact Linear Collider damping rings", *Phys. Rev. ST. Accel. Beams*, vol. 17, no. 7, Jul. 2014. `doi:10.1103/physrevstab.17.071003`

[11] J. H. Billen and L. M. Young, "Poisson superfish", LANL, New Mexico, USA, Rep. LA-UR-96-1834, 2000.

[12] O. Kononenko, L. Ge, C. Ko, Z. Li, C.-K. Ng, and L. Xiao, "Advances in Massively Parallel Electromagnetic Simulation Suite ACE3P", in *Proc. 12th Int. Computational Accelerator Physics Conf. (ICAP'15)*, Shanghai, China, Oct. 2015, pp. 183–187. `doi:10.18429/JACoW-ICAP2015-FRAJI3`

[13] NERSC, http://www.nersc.gov/.